Modelling the seasonal dynamics of marine plankton in the southern Baltic Sea. Part 1. A Coupled Ecosystem Model*

OCEANOLOGIA, 47 (4), 2005.
pp. 591–619.

KEYWORDS
Ecosystem model
Nutrients
Phytoplankton
Microzooplankton
Pseudocalanus elongatus
Clupea harengus

Lidia Dzierzbicka-Głowacka

Institute of Oceanology,
Polish Academy of Sciences,
Powstańców Warszawy 55, PL–81–712 Sopot, Poland;

e-mail: dzierzb@iopan.gda.pl

Received 6 October 2005, revised 25 November 2005, accepted 1 December 2005.

Abstract

The paper presents a one-dimensional Coupled Ecosystem Model (1DCEM) consisting of three submodels: a meteorological submodel for the physics of the upper layer and a biological submodel, which is also driven by output from the physical submodel. The biological submodel with a high-resolution zooplankton module and a simple prey-predator module consists of seven mass conservation equations. There are six partial second-order differential equations of the diffusion type for phytoplankton, microzooplankton, mesozooplankton, fish, and two nutrient components (total inorganic nitrogen and phosphate). The seventh equation, an ordinary differential equation, describes the development of detritus at the bottom. In this model the mesozooplankton (herbivorous copepods) is represented by only one species – *Pseudocalanus elongatus* – and is composed of 6 cohorts. The fish predator is represented by 3 cohorts of early juvenile herring *Clupea harengus*. Hence, the biological submodel consists of an additional twelve equations, six for weights and six for the numbers in 6 cohorts of *P. elongatus*, and

---

* This research was carried out as part of the statutory programme of the Institute of Oceanology in Sopot, Poland (No II.1.4) and was supported by the Polish State Committee of Scientific Research (grant No 2P04F 075 27, 2004–2006).

The complete text of the paper is available at http://www.iopan.gda.pl/oceanologia/

three equations for the biomasses of 3 predator cohorts. This model is an effective tool for solving the problem of ecosystem bioproductivity and was tested in Part 2 for one partcular year.

1. Introduction

The numerous threats and natural disasters elicited by changes in the environment have persuaded experts to radically intensify ecological investigations and forecasts on a regional and global scale. A key part in these changes is played by marine ecosystems, especially the organic matter production processes occurring in them. Marine production is the most important mechanism of carbon exchange between the sea and the atmosphere, and therefore requires to be monitored continuously with traditional methods (from on board ship), as well as with modern remote sensing techniques. This kind of research is extremely expensive and demands the cooperation of interdisciplinary study groups working both in laboratories and on board ship. Nevertheless, effective monitoring of marine production is practically impossible with traditional methods. During the last 20 years, another way of solving these problems has been developed using numerical methods describing the bioproductivity of marine basins.

Good reviews of coastal marine ecosystem modelling have been published by Fransz et al. (1991, 1998). Ecological modelling of the Baltic Sea began at the end of the 1960s with material balance models (see e.g. Fonselius 1969). The first general conceptual ecosystem model of the Baltic Sea was presented by Jansson (1972). Practical simulations of the Baltic Sea ecosystem have been carried out Stigebrandt & Wulff (1987), Savchuk et al. (1988), Ennet et al. (1989), Tamsalu & Ennet (1995), Svansson (1996), Ołdakowski & Renk (1997), Tamsalu (1998), Dzierzbicka-Głowacka (2000) and Marmefelt et al. (2002). Models with a high-resolution zooplankton module should also be included: Carlotti & Radach (1996), Carlotti & Wolf (1998), Fennel (2001) and Dzierzbicka-Glowacka (2005).

The application of turbulent diffusion equations to the modelling of concentrations of herbivorous zooplankton, which in turn are fed upon by larval fish and carnivorous Copepoda, is a task more complex than the modelling of hydrodynamically passive phytoplankton. Considering the minute sizes of this zooplankton, we can assume, without committing too serious an error, that turbulent mixing affects ambush-type microzooplankton in the same way as phytoplankton. However, when modelling zooplankton with a cruise-type behaviour, this assumption has to be rejected, because they are capable of active movement. Relations with predators hunting for zooplanktonic prey are more complex and the foraging process as a component of the source function cannot be defined in the same way as that of phytoplankton, because the principal factor governing it is the encounter rate between predator and prey (Rothschild & Osborn 1988, Evans 1989, Sundby & Fossum 1990, Kiørboe 1993, Kiørboe & MacKenzie 1995, Kiørboe & Saiz 1995, MacKenzie & Kiørboe 1995, Caparroy & Carlotti 1996, Dower et al. 1997, Dzierzbicka-Głowacka, in press).

The main objective of the present paper is to construct a new and considerably more complex model than the previous physical and biological model for describing marine production in the southern Baltic Sea (see Dzierzbicka-Głowacka 2005), hence to build a $1D$-Coupled Ecosystem Model ($1D$CEM) as a tool suitable for studying the annual, seasonal, monthly and daily variability of plankton in the southern Baltic Sea. The model enables natural resources to be assessed and also simplifies the forecasting of fishing limits. The Baltic Sea fishery is based to a high degree on planktivorous fish such as the sprat (*Sprattus sprattus*) and herring (*Clupea harengus*), which feed on herbivorous copepods such as *Pseudocalanus elongatus*.

This $1D$CEM model consists of three submodels – meteorological, physical and biological: the meteorological one caters for the physics of the upper layer, while the biological one is also driven by output from the physical submodel. The biological submodel, which simulates the temporal changes in phytoplankton, microzooplankton and the two nutrient components (total inorganic nitrogen and phosphate), is coupled with a copepod model and a simple prey-predator model. The copepod model for *P. elongatus* links trophic processes to population dynamics and simulates individual growth within 6 cohorts representing the successive growth stages, as well as the changes in biomass between cohorts. The predator is represented by 3 cohorts of early juvenile herring *C. harengus*, whose growth rate is controlled by the encounter rate between consumer and prey. The predator is introduced in the model as a top regulator that may play a significant role in marine ecosystems. The $1D$CEM was tested for the wide range of variability in the physical, biological and chemical parameters measured in the sea. The numerical simulations made for one year are presented in Part 2.

In Part 1, section 2 describes the combined marine ecosystem model, and subsection 2.1 presents the concept of the model. The three components of $1D$CEM involving the biology, physics and meteorology together with the boundary and initial conditions are presented in 2.2, 2.3 and 2.4 respectively. In Part 2, the forcing functions are described in section 2 and the data for the simulation studies are given in section 3. The main part of the paper, the numerical results, is presented in section 4, whereas the data from experiments and simulations are compared in section 5, before they are finally discussed in section 6.

2. Marine ecosystem model

A model of the marine system is an excellent way to formalize and test knowledge of a complex aquatic ecological system and to solve the problem of how to manage rationally our living marine resources in the future. The marine system model consists of two parts: a hydrodynamic one and an ecosystem one. The equations are in the course of development.

Modelling of the ecosystem part has tended to concentrate on two trophic levels – the phytoplankton and the fish. In the former case this has been possible because the plant material was considered conceptually and measured analytically as a single unit. In the latter case the major commercial fish species were treated one by one, mainly in relation to the effects of fishing effort on stock abundance, since the fishing industry supplied the necessary data.

It has been the usual practice to included herbivores or benthic detritus feeders in model simulations only as a means of supplying or disposing of biological matter required by those parts of the ecosystem that the model treats as central components. As far as the benthos is concerned there is, so far, no evidence of a change in this approach, and the zooplankton are at present regarded as mere consumers rather than as organisms having certain patterns of growth, reproduction and mortality. Thus, the parameters of population dynamics – fecundity, age structure, age birth and death rates – are more important in determining the behaviour of an ecosystem than the simpler concepts of organic matter flow.

There are still, however, certain limitations which must be imposed here. Zooplankton are a very heterogeneous group, defined rather by the method of collection than by their position in the food web. Any net haul, and particularly a series of hauls with different mesh sizes, is likely to contain bacteriovorous, herbivorous, omnivorous, and carnivorous species. Yet nearly all models incorporating zooplankton consider the entire catch as herbivores feeding in the upper layers of the sea. There are good reasons for this: herbivorous copepods are the largest group of the zooplankton, processing as they do nearly all of the primary production. In turn, they (or their faeces and excreta) are the predominant source of food for the rest of the system.

The marine ecosystem model consists of a set of equations. These are all of the same general form, i.e. equations of the diffusion type, expressing changes in any state variable.

The intention is to simulate the production of marine plankton by using biological dynamics within a physical environment that is as realistic as possible without making the model components too different in complexity. Therefore two 1*D* submodels have been used: first, an upper layer model for simulating the development and decay of the seasonal thermocline, and a second one for the development and decay of the annual biological production. The meteorological component drives both 1*D* models, and the output of the physical submodel is also used for driving the biological submodel, whose output, in turn, is used in the physical submodel (see subsection 2.3) (Fig. 1).

The meteorological component calculates the forcing functions for the physical oceanographic and biological components. Wind stress, global radiation and the heat balance at the sea surface are determined from standard meteorological observations. Global radiation is calculated by adapting and applying a radiation model that is based on the radiation

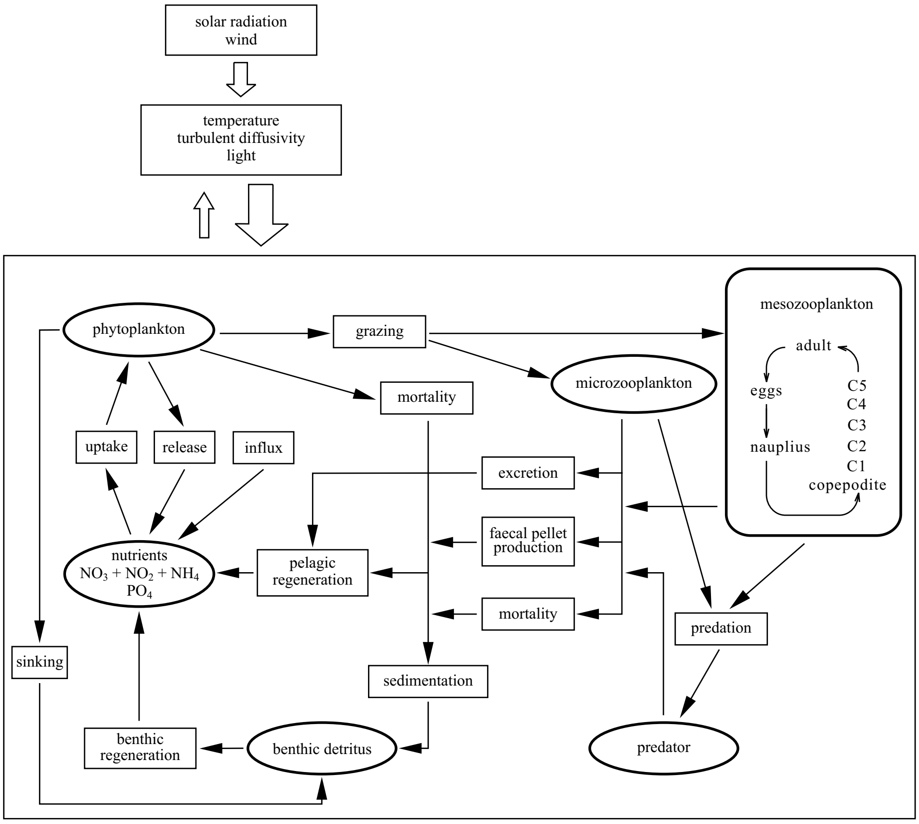

Fig. 1. Conceptual diagram of the coupled model

in the outer atmosphere and on local cloudiness. The latent and sensible heat fluxes are calculated by so-called bulk formulae.

The physical upper layer model simulates the formation and decay of the seasonal thermocline and the vertical turbulence structure on small time scales by impressing temporal small scale meteorological variability at the sea surface. The turbulence profiles serve to mix the biological and chemical constituents in the biological model.

The biological upper layer model consists of seven mass conservation equations. There are six diffusion advection reaction equations for phytoplankton, micro- and mesozooplankton, predator biomass and two nutrients in the water column. The seventh equation, an ordinary differential equation, describes the development of detritus at the bottom. The model takes into account those physical, biological and chemical processes (selected from the subject literature) that exert the most decisive influence on the variability of the characteristics investigated.

The various components will now be elucidated, but in the reverse order.

2.1. Concept

The coupled ecosystem model is essentially a point model, that is, only a single point in space is considered. Here, the horizontal, quasi-homogeneous upper layers of the study areas will be examined from the standpoint of the areas' boundary layer dynamics. Thus, all horizontal gradients vanish. It is assumed that all the hydrochemical and hydrobiological characteristics remain unchanged in the horizontal plane. Fundamental to the present modelling study is the assumption of an absolutely stable vertical distribution of the average sea water density. Differential upper layer models are probably better suited than integral models to the purpose of coupling the biological upper layer dynamics to the physical dynamics while maintaining the interactions of the vertical structures. Initially, six state variables are taken into consideration: limiting nutrients $\{Nutr\}$, phytoplankton $\{Phyt\}$, microzooplankton $\{Z_{micro}\}$, mesozooplankton $\{Z_{meso}\}$, predator $\{B\}$ and detritus $\{Detr\}$. The temporal changes of the state variables are completely described by the dynamics of the biological and chemical sources and sinks.

The philosophy is to make the model as simple as possible as far as phytoplankton is concerned: phytoplankton is modelled with the aid of only one state variable. Phytoplankton naturally consists of many different species, each with different dynamic characteristics and contributing different proportions of biomass during the year. The assumption in using the phytoplankton biomass is that the species composition regulates itself according to nutrient availability. Thus, we are assuming that the dynamic constants used are representative of the whole phytoplankton community. The phytoplankton concentration is taken as a dynamically passive physical quantity, i.e. it is incapable of making autonomous movements, and will henceforth be represented by the carbon concentration.

The biological model incorporates formulations of the primary production mechanism and of the remineralization mechanisms within the mixed layer in the lower layers and at the bottom. Phytoplankton in the water is either grazed by zooplankton or else it dies and sinks. The grazed phytoplankton can be divided into three groups: one contributes to zooplankton growth, another is deposited as faecal pellets, and a third is excreted by the zooplankton as dissolved metabolites, thus replenishing the nutrient pool. A proportion of the material contributing to growth is assumed to be lost – this represents dying zooplankton and predation. Proportions of both faecal and excreted material are immediately regenerated. In turn, zooplankton is subject to predation by early juvenile fish, giving rise to its growth through the prey-predator encounter rate.

In this model nutrients are represented by two components: total inorganic nitrogen ($NO_3 + NO_2 + NH_4$) and phosphate (PO_4). The nutrients serve both as a trigger and as a limiting agent for primary production. The Redfield ratio is applied.

The concept of the detrital pool at the bottom has been introduced to create a lag in the remineralization of the majority of detritus and the eventual replenishment of the upper layer with nutrients. This complex process is parameterized by assuming a net remineralization rate for bottom detritus (Billen et al. 1991).

One state variable for microzooplankton was considered. Microzooplankton is defined as heterotrophic planktonic organisms from 10 to 500 μm SED (Spherical Equivalent Diameter), excluding heterotrophic nanoflagellates and naupliar/larval stages of larger zooplankton and of benthic organisms. The microzooplankton consists of ciliates and other heterotrophic protists, which are filter-feeders, feeding on phytoplankton. Represented as passive particles, the microzooplankton is assumed to be speedless. This is not realistic, but its speed is very, very small – c. 0.5 body length. Therefore, the speed of microzooplankton can be assumed to be zero.

In this paper the mesozooplankton (herbivorous copepods) has been introduced into this model as animals having definite patterns of growth, reproduction and mortality. The assumption is that only one species of copepod (*P. elongatus*) is present. The population is represented by six cohorts in different developmental stages, hence a second simplification is assumed, namely, that recruitment of the next generation occurs after a fixed period of adult life. Here, adults and copepodites are assumed to survive the winter. The copepod *P. elongatus* is one of the more abundant zooplankton species in the Baltic. In the Gdańsk Deep this species occurs in great abundance: in deeper layers, below 30 m, it becomes the dominant representative of the mesozooplankton, and below the isohaline layer, almost the only one.

The predator is represented by 3 cohorts of early juvenile herring *C. harengus* of the 4–10 cm size class. Spring spawning herring stocks occur normally as components of the pelagic fish community in the Baltic Sea and adjacent waters. The Vistula Lagoon is an important spawning area for southern Baltic spring-spawning herring *C. harengus.* At the turn of winter and spring (in March), adults migrate from the southern Baltic to the spawning grounds in the shallow, brackish water of the Vistula Lagoon (Fey 2001). Herring in the Vistula Lagoon has three cohorts each year (Margoński 2000). Herring larvae (> 5 mm long) appear in plankton samples at the beginning of April. When young herring are about 40 to 50 mm long, they undergo metamorphosis, after which they are identified as juveniles. Metamorphosis in the Vistula Lagoon begins in June. Early juvenile herrings migrate out of the Polish part of the Vistula Lagoon: those of the first cohort at the end of June, the second cohort in July, and the third cohort in August. These early juveniles (c. 40 mm) appear in the Gulf Gdańsk after two weeks. They feed on a variety of zooplankton, copepods being the most important prey throughout the year. The predator biomass reflects prey availability through growth and mortality rates.

The phytoplankton standing stock, zooplankton, early juvenile fish and nutrients in the water column serve as time- and depth-dependent pools. Detritus is a time-dependent pool at the bottom. All pools are prognostic state variables. Bacteria are not explicitly simulated as prognostic variables. Their activity only appears implicitly in the parameterizations of the remineralization terms. Benthic detritus accumulates by sinking out of the water column. It is regenerated by bacterial action, and the resulting nutrients move upwards by turbulent diffusion.

2.2. Biological submodel

The biological model comprises seven state variables: nutrients (total inorganic nitrogen and phosphate), phytoplankton, microzooplankton, mesozooplankton (*P. elongatus*), fish predator (early juvenile herring) and benthic detritus (see Fig. 1).

The system of equations in the biological submodel consists of six nonlinearly coupled second-order partial differential equations, two equations for nutrients, one equation for phytoplankton, two for zooplankton (micro- and meso-), one for the predator and one ordinary first-order differential equation for benthic detritus, together with the initial and boundary conditions.

This model is assumed to be governed by the following set of equations:

$$\begin{aligned}\frac{\partial\{Nutr_P\}}{\partial t} &= \frac{\partial}{\partial z}\left(K_z\frac{\partial\{Nutr_P\}}{\partial z}\right) - \mathrm{UPT}_P + F_{inf,P} + \mathrm{REL}_P + \\ &+ \mathrm{REMI}_P + \mathrm{EXC}_P, \end{aligned}\tag{1}$$

$$\begin{aligned}\frac{\partial\{Nutr_N\}}{\partial t} &= \frac{\partial}{\partial z}\left(K_z\frac{\partial\{Nutr_N\}}{\partial z}\right) - \mathrm{UPT}_N + F_{inf,N} + \mathrm{REL}_N + \\ &+ \mathrm{REMI}_N + \mathrm{EXC}_N, \end{aligned}\tag{2}$$

$$\begin{aligned}\frac{\partial\{Phyt\}}{\partial t} + w_z\frac{\partial\{Phyt\}}{\partial z} &= \frac{\partial}{\partial z}\left(K_z\frac{\partial\{Phyt\}}{\partial z}\right) + \mathrm{PRE} - \\ &- \mathrm{RES} - \mathrm{MOR}_P - \mathrm{GRA}, \end{aligned}\tag{3}$$

$$\begin{aligned}\frac{\partial\{Z_{micro}\}}{\partial t} &= \frac{\partial}{\partial z}\left(K_z\frac{\partial\{Z_{micro}\}}{\partial z}\right) + \mathrm{ING}_Z - \mathrm{FEC}_Z - \mathrm{MET}_Z - \\ &- \mathrm{MOR}_Z - \mathrm{PRED}_Z, \end{aligned}\tag{4}$$

$$\frac{\partial\{Z_{meso}\}}{\partial t} = \frac{\partial}{\partial t}\left(\sum_{i=1}^{6} W_i Z_i\right), \tag{5}$$

$$\frac{\partial\{B\}}{\partial t} = \frac{\partial}{\partial t}\left(\sum_{i=1}^{3} B_i\right), \tag{6}$$

$$\frac{d\{Detr\}}{dt} = -F_P(H) + \mathrm{D} - \mathrm{REMD}. \tag{7}$$

If it is assumed that mesozooplankton (*P. elongatus*) is composed of 6 cohorts of copepods with weights W_i and numbers Z_i (where $Z_{meso} = \sum W_i Z_i$), then the biological submodel contains an additional twelve equations, six equations for weights and six equations for the numbers in 6 cohorts of *P. elongatus*:

$$\frac{\partial W_i}{\partial t} = \mathrm{ING}_i - \mathrm{FEC}_i - \mathrm{MEF}_i, \tag{8}$$

$$\frac{\partial Z_i}{\partial t} = \frac{\partial}{\partial z}\left(K_z\frac{\partial Z_i}{\partial z}\right) - \mathrm{MIG}_i - \mathrm{MOR}_i - \mathrm{PRED}_i. \tag{9}$$

However, the predator (early juvenile herring *C. harengus*) is composed of 3 cohorts; hence, the biological submodel further includes three equations for the biomasses of the 3 predator cohorts B_i (where $B = \sum B_i$):

$$\frac{\partial B_i}{\partial t} = \frac{\partial}{\partial z}\left(K_z\frac{\partial B_i}{\partial z}\right) + g_{B_i}B_i - \mathrm{PRED}_{P_i}. \tag{10}$$

The origin of the Cartesian coordinate system is set at the surface of the sea basin with the z-axis directed upwards, w_z denotes the sinking velocity of phytoplankton, and K_z represents the turbulent diffusion coefficient determined by Peters et al. (1988) as

$$K_z = 5 \times 10^{-4}(1+Ri)^{-2.5} + 10^{-6}, \tag{11}$$

for the upper layer of a stratified sea down to a depth of 100 m, i.e. to a depth of more than twice the thickness of the euphotic layer. The biochemical terms used in eqs. (1)–(11) are listed below. A list of the symbols used in the biological model is given in Appendix 1.

2.2.1. Phytoplankton

The phytoplankton biomass $\{Phyt\}$ is affected by primary production PRE, respiration RES, mortality MOR$_P$, and grazing by zooplankton GRA. The primary production PRE (eq. (12)) is calculated from the light limitation function d_I, the nutrient minimum from the total inorganic nitrogen and phosphate limitation functions d_N and d_P (eq. (13)), and the assimilation number d_A; d_A is the maximum photosynthetic rate, i.e. the ratio of production (amount of assimilated carbon) to the chlorophyll concentration, and for the Gdańsk Deep is described as a function of temperature (eq. (15)) (Renk & Ochocki 1998). d_I is used to calculate the photosynthetic rate for the saturation irradiance E_{opt} (the irradiance at which the rate of photosynthesis is highest) (eq. (14)) and the irradiance at depth z, E (eq. (16)). The underwater light intensity E is dependent on the photosynthetically available irradiation PAR E_o and the irradiance transmission coefficient $T(z)$ as a function of K_d, the sum of components responsible for the attenuation of irradiance by pure water, phytoplankton and other optically active admixtures, which was calculated from Woźniak's bio-optical classification of natural waters (eq. (17)) (Woźniak & Pelevin 1991). For nutrient limitation the Michaelis-Menten formula is applied with k_{Nutr} as the half-saturation constant (eq. (13)). Metabolic processes in plants are accompanied by catabolic processes such as respiration. Therefore, the true net increase in primary production, i.e. in the phytoplankton biomass, per time unit is reduced by the losses due to respiration (Parsons et al. 1977). Respiration RES consists of basic and photo-respiration (eq. (19)), each being proportional to the phytoplankton biomass $\{Phyt\}$ (Ryther 1956, Parsons et al. 1984). The basic dark respiration rate is m_P^n, a factor proportional to the maximum photosynthetic rate (Ryther 1956), and the photo-respiration rate is m_P^d, a factor proportional to the rate of primary production (Radach & Moll 1993). The temperature dependence m_P^T is modelled according to eq. (20), where the constant m expresses the rate of change of respiratory rate m_P^T with temperature

– this doubles for a temperature increase of $T_o = 10°\text{C}$ and $m_P^T(T_o) = 1$ (Riley 1946). The natural phytoplankton mortality MOR_P is a process which results in some losses in biomass. It was assumed that mortality is directly proportional to the phytoplankton biomass $\{Phyt\}$ (Raymont 1980, Sjöberg 1980) with a mortality rate of m_P (eq. (21)). Phytoplankton grazing by zooplankton GRA is assumed to be proportional to the microzooplankton and herbivorous copepod biomass ($Z = \{Z_{micro}\} + \{Z_{meso}\}$) at a rate of $f(\{Phyt\})$ (eq. (22)), but this rate is a function of the phytoplankton biomass with a threshold $\{Phyt\}_0$, below which grazing ceases, and of the half-saturation constant k_{Phyt}, where $g_{\max}$ denotes the maximum grazing rate (eq. (23)) (Steele & Mullin 1977).

$$\text{PRE} = d_A\, d_I \min\{d_N, d_P\}\{Phyt\}, \tag{12}$$

$$\begin{aligned} d_I &= \frac{E}{E_{opt}} \exp\left(1 - \frac{E}{E_{opt}}\right), \quad d_N = \frac{\{Nutr_N\}}{\{Nutr_N\} + k_{Nutr\,N}}, \\ d_P &= \frac{\{Nutr_P\}}{\{Nutr_P\} + k_{Nutr\,P}}, \end{aligned} \tag{13}$$

$$E_{opt} = 313.64 + 19.56\,T, \tag{14}$$

$$d_A = 1.385 + 0.238\,T, \tag{15}$$

$$\begin{aligned} E &= E_o T(z) = E_o \exp\left(\int_0^z -\overline{K_d(z)}dz\right), \\ \overline{K_d(z)} &= 1/300 \int_{400\ \text{nm}}^{700\ \text{nm}} K_d(z,\lambda)d\lambda, \end{aligned} \tag{16}$$

$$\begin{aligned} K_d(z,\lambda) &= K_w + \text{Chl}\,a\{C_1(\lambda)\exp\left[-a_1(\lambda)\text{Chl}\,a\right] + \\ &+ K_{d,i}(\lambda)\} + \Delta K(\lambda), \end{aligned} \tag{17}$$

$$\Delta K(\lambda) = 0.068 \exp\left[-0.0149(\lambda - 550)\right], \tag{18}$$

$$\text{RES} = \text{RES}_n + \text{RES}_d = d_A \left(m_P^n + m_P^d \min\{d_I, d_N\}\right)\{Phyt\}, \tag{19}$$

$$m_P^T = \exp\{m(T - T_o)\}, \tag{20}$$

$$\text{MOR}_P = m_P\{Phyt\}, \tag{21}$$

$$\text{GRA} = f(\{Phyt\})\left[\{Z_{micro}\} + \{Z_{meso}\}\right], \tag{22}$$

$$\begin{aligned} f(\{Phyt\}) &= g_{\max}\frac{\{Phyt\} - \{Phyt\}_0}{\{Phy\} - \{Phyt\}_0 + k_{Phyt}} \\ &\quad \text{for} \quad \{Phyt\} > \{Phyt\}_0. \end{aligned} \tag{23}$$

2.2.2. Microzooplankton

The temporal changes in the microzooplankton biomass $\{Z_{micro}\}$ are caused by ingestion ING_Z, microzooplankton faecal pellets FEC_Z, metabolism MET_Z, mortality MOR_Z and predation PRED_Z. The ingestion rate ING_Z is defined as in the case of phytoplankton grazing (eq. (24)), i.e. it is assumed to be proportional to the microzooplankton biomass $\{Z_{micro}\}$ at a rate $f(\{Phyt\})$ with a maximum ingestion rate $f_{\max}$ (eq. (25)). The total rate of metabolic loss MET can be split into three components with different relations to the food uptake rate ING. M_s is assumed to be the resultant or basic metabolism, independent of food supply. The respiratory costs of foraging for and capturing food M_r should fall as the food concentration and, correspondingly, $f(\{Phyt\})$, rises. Finally, there is the cost of assimilating and biochemically transforming the food (specific dynamic action, M_a), proportional to A (eq. (26)) (Steele & Mullin 1977). Faecal pellet production and carcasses of microzooplankton are described by eq. (27) with the percentage of ingestion egested as faecal material n_f and ending up as dead microzooplanktom n_Z. However, the intensity of predation PRED_Z (eq. (28)) depends on the predator biomass through the coefficient $\alpha\, g_B$, where g_B is the predator growth rate and α is assumed to be 5/3; this means that 60% of ingested food contributes to predator growth and 40% is voided as faecal pellets, and excreted material is regenerated immediately.

$$\mathrm{ING}_Z = f(\{Phyt\})\{Z_{micro}\}, \tag{24}$$

$$f(\{Phyt\}) \;=\; f_{\max}\frac{\{Phyt\}-\{Phyt\}_0}{\{Phyt\}-\{Phyt\}_0+k_{Phyt}} \quad \text{for} \quad \{Phyt\}>\{Phyt\}_0, \tag{25}$$

$$\mathrm{MET}_Z = M_s + M_r + M_a = M_s + n_e A_Z, \quad A_Z = n_a \mathrm{ING}_Z, \tag{26}$$

$$\mathrm{FEC}_Z = n_f \mathrm{ING}_Z, \quad \mathrm{MOR}_Z = n_z \mathrm{ING}_Z, \tag{27}$$

$$\mathrm{PRED}_Z = \alpha\, g_B\{B\}. \tag{28}$$

2.2.3. Mesozooplankton as animals

The changes in weight W_i and number Z_i of an individual copepod are caused by ingestion ING_i, zooplankton faecal pellets FEC_i, metabolism MET_i, mortality MOR_i and predation PRED_i as well as diurnal migration MIG_i. The ingestion rate ING_i is defined as the rate of food intake per unit time per animal, the coefficient of food selection being given by τ (eq. (29)). This is a function of the food concentration $\{Phyt\}$ (eq. (30)), temperature T, and the animal's weight W_i, and takes the value of $\alpha = 2/3$ (Paffenhöfer 1971). The rate of assimilation A is computed as a constant fraction of the ingestion rate (eq. (31)) (e.g. Steele (1974) who used $A_i = 0.7\mathrm{ING}_i$). The major metabolic loss of organic matter from a population is undoubtedly through respiration. The total rate of metabolic loss MET is defined as in the case of microzooplankton. The number of juveniles is defined on the assumption that eggs are released by the adult female as a single brood, continuously throughout some time span J. The simplest assumption is that the female, instead of utilizing assimilated food for growth, uses it for egg production. However, the males feed at the same rate as females and do not produce eggs. The average number of eggs produced per day by one female, EGG, is obtained here as a function of the maximum growth rate, g_Z, i.e. by multiplying exp $g_Z - 1$ from the equation for the growth rate by $W_{\mathrm{female}}/W_{\mathrm{egg}}$ (eq. (32)) (Dzierzbicka-Głowacka, in press). Detailed descriptions of the growth, development and egg production for some geographically separate populations of *Pseudocalanus* are given in Dzierzbicka-Głowacka (2004a,b) and Dzierzbicka-Głowacka & Zieliński (2004). The efficiency term X is the conversion of the biomass increase in the adult population into eggs, including the 'wasted' growth in the males. The intensity of mortality MOR_i depends on numbers Z_i in the individual cohorts and the average mortality rate m_z, which is given by Klein Breteler et al. (1995) (eq. (33)) for different food concentrations and temperatures. The vertical migration is conceived in this work on the assumption that (i) migration is described in a day-night cycle, and (ii) the vertical distribution of zooplankton is described by the function $f(z)$. Consequently, the diurnal migration can be described as eq. (34), where $f(z) = -0.0003775z^2 + 0.62$, a_w is the relative amplitude of zooplankton concentration changes, t_o is the time in which the maximum zooplankton concentration occurs. PRED_i represents the losses incurred by Z_i as a result of predation (eq. (35)). Its magnitude can be determined from the biomass of predator on the assumption that the loss incurred by the prey concentration is proportional to the increase in predator biomass which is reduced to $\alpha\, g_B$, where $\alpha = 5/3$ as in the case of microzooplankton. The body length of copepods was computed from the weight – length relationship of *Pseudocalanus* $W = 11.9L^{3.64}$ (Corkett & McLaren 1978).

$$\mathrm{ING}_i = \tau fil_i(\{Phyt\})t_1 t_2^T W_i^{\alpha}, \quad \mathrm{ING} = \sum_i \mathrm{ING}_i, \tag{29}$$

$$fil_i(\{Phyt\}) = fil_{i_{\max}} \frac{\{Phyt\} - \{Phyt\}_0}{\{Phyt\} - \{Phyt\}_0 + k_{Phyt}} \quad \text{for} \quad \{Phyt\} > \{Phyt\}_0, \tag{30}$$

$$\mathrm{MET}_i = M_s + M_r + M_a = M_s + n_e A_i, \quad A_i = n_a \mathrm{ING}_i,$$

$$\mathrm{MET} = \sum_i \mathrm{MET}_i, \tag{31}$$

$$\mathrm{EGG} = W_{\mathrm{female}}/W_{\mathrm{egg}}(\exp\, \mathrm{g_Z} - 1), \quad \mathrm{EGG}_{prod} = X \int_J \mathrm{EGG}dt, \tag{32}$$

$$\mathrm{MOR}_i = m_z Z_i, \quad \mathrm{MOR} = \sum_i \mathrm{MOR}_i, \tag{33}$$

$$\mathrm{MIG}_i = \{1 + a_w \cos(\omega(t - t_o)) f_z\} \frac{\partial Z_i}{\partial z}, \tag{34}$$

$$\mathrm{PRED}_i = \alpha\, g_B\, \{B\}/W_i. \tag{35}$$

2.2.4. Predator

The predator biomass of each cohort is defined by the growth rate of the predator g_{B_i} and predation (=mortality) PRED_{P_i}. The predator growth rate, when the predator is food limited, is linearly related to the encounter rate E by eq. (36), where g_1 is the proportionality parameter between growth rate and encounter rate and g_2 is the constant growth rate term. An increased encounter rate only leads to increased growth when the predator is food limited and then $g_1 E$ has a decisive influence on growth rate; if the mean time between prey encounters becomes small, the predator growth rate becomes limited not by prey availability (E is greater than 1 s^{-1} and is unlikely to lead to an increased ingestion rate, and then $g_1 E$ is constant) but by the parameter g_2, and then g_2 and $g \to g_{\max}$ takes on a predominant significance. The encounter rate between predator and prey, $E = E_B + E_T$, is governed by two kinds of processes – behavioural and hydrodynamic – resulting from the interacting movements of water masses. E can be derived from eq. (37) (Rothschild & Osborn 1988, Kiørboe & Saiz 1995, Seuront et al. 2001). E is determined by the predator's contact radius d, i.e. the maximum distance at which the predator can perceive prey, the linear orbital velocity of turbulent eddies w and prey concentration $Z = \{Z_{micro}\} + \{Z_{meso}\}$, under the assumption that the speed of the predator v exceeds that of the prey u. Laurence (1985) determined the perception distance for larval haddock as a function of body length d_o by $d = 2/3\pi(0.75 d_o)^2$. However, Miller et al. (1988) defined the high estimate of swimming speed of a predator as $\log v = 1.07 \log d_o - 1.11$. The size of the predator was computed following the procedure:

$d_1 = d_o + d g_d$ after 1 day ...

$d_i = d_{i-1} + d_{i-1} g_d$ after i days

$d_{i+1} = d_i + d_i g_d$ after $i + 1$ days assuming that the initial size of an individual in each cohort is $d_o = 40$ mm and g_d is the mean growth rate in length. The turbulent velocity w was given by Rothschild & Osborn (1988) as eq. (38), where ε is the dissipation rate of turbulent kinetic energy and l is the characteristic length scale of turbulent eddies. Here it is assumed that the characteristic length scale is defined as the predator's reactive distance; hence the separation distance between predator and prey is also the perceptive distance of the predator, i.e. $l = d$ in equation for encounter rate E.

$$g = \begin{cases} g_1 E + g_2 & \text{for} \quad 0 < Z < Z_{\max} \\ g_{\max} & \text{for} \quad Z \geq Z_{\max}, \end{cases} \tag{36}$$

$$\begin{aligned} E &= E_1 + E_2, \quad E_1 = \pi Z_{micro}\, d^2 \frac{3v^2 + 4w^2}{[3(v^2 + w^2)]^{0.5}}, \\ E_2 &= \pi Z_{meso}\, d^2 \frac{u^2 + 3v^2 + 4w^2}{[3(v^2 + w^2)]^{0.5}}, \end{aligned} \tag{37}$$

$$w = 1.9(\varepsilon l)^{1/3}, \quad \varepsilon = A_z \left(\frac{\partial \overline{u}}{\partial z} \right)^2. \tag{38}$$

2.2.5. Nutrients

The nutrient concentration $\{Nutr\}$ is determined by algal uptake UPT, nutrient influx F_{inf}, remineralized dead phytoplankton, zooplankton faecal pellets and dead zooplankton REMI, and by zooplankton excretion EXC and nutrient release REL. Respiration in the dark consumes particulate organic matter. For matter to be conserved, the respiration term in the equation for phytoplankton must be balanced by a nutrient release term REL in the equations for nutrients (P and N). This term parameterizes the contribution of respiration to the nutrient pool, assuming a fixed P:C ratio in the equation for phosphate ($g = g_P$) and N:C ratio in the equation for total inorganic nitrogen ($g = g_N$) (eq. (39)). Nutrient uptake by phytoplankton cells UPT is assumed to occur for positive net production only and for photo-respiration (eq. (40)). Excretion of dissolved and particulate material is parameterized via the amount of grazed material. Soluble zooplankton excretion EXC is parameterized by the metabolism costs MET (eq. (41)) with the percentage of ingestion n_e regenerated as soluble zooplankton excreta. The total faecal pellet production FEC (eq. (42)), along with the percentage of ingestion n_f was evaluated as faecal material. Remineralization REMI within the water column by the 'microbial food web' is assumed for proportions of dead phytoplankton REMP (eq. (44)), dead (micro- and meso-) zooplankton and the early juveniles of fish REMZ (eq. (45)) and faecal pellets REMF (eq. (46)), with the percentages p_m, p_z and p_f corresponding to the components of dead phytoplankton, dead zooplankton, and fish and faecal material, which are immediately recycled in the water column (eq. (47)) (Radach & Moll 1993, Dzierzbicka-Głowacka & Zieliński 1997a,b). The nutrient influx vertical was used as an exponential function of depth (eq. (48)) (Jędrasik & Kowalewski 1993).

$$\mathrm{REL} = g\mathrm{RES}, \tag{39}$$

$$\mathrm{UPT} = g(\mathrm{PRE} - \mathrm{RES}), \tag{40}$$

$$\begin{aligned} \mathrm{EXC} &= \mathrm{EXC}_T + \mathrm{EXC}_B, \quad \mathrm{EXC}_T = g(\mathrm{MET}_Z + \mathrm{MET}), \\ \mathrm{EXC}_B &= g\frac{1}{3}g_B\{B\}, \end{aligned} \tag{41}$$

$$\mathrm{FEC}_T = n_f(\mathrm{ING}_Z + \mathrm{ING}), \quad \mathrm{FEC}_B = \frac{1}{3}g_B\{B\}, \tag{42}$$

$$\mathrm{MOR}_T = n_z(\mathrm{ING}_Z + \mathrm{ING}), \quad \mathrm{MOR}_B = m_B\{B\}, \tag{43}$$

$$\mathrm{REM}P = p_p\mathrm{MOR}_P, \tag{44}$$

$$\mathrm{REM}Z = p_z[\mathrm{MOR}_T + \mathrm{MOR}_B], \tag{45}$$

$$\mathrm{REM}F = p_f[\mathrm{FEC}_Z + \mathrm{FEC}_B], \tag{46}$$

$$\mathrm{REMI} = g(\mathrm{REM}P + \mathrm{REM}Z + \mathrm{REM}F), \tag{47}$$

$$F_{inf} = F_{inf,o}\exp(-0.1\,z). \tag{48}$$

2.2.6. Benthic detritus

Benthic detritus $\{Detr\}$ varies according to the input of algal detritus from the water column D, and loss by remineralization at the bottom REMD. Remineralization REMD is assumed proportional to the amount of benthic detritus available $\{Detr\}$ (eq. (50)), where r_d denotes the remineralization rate of benthic detritus (Radach et al. 1984). The detrital material sedimenting out of the water column D consists of contributions from dead phytoplankton, faecal pellets and dead zooplankton and early juveniles of fish, which are not remineralized in the water column (eq. (49)).

Sedimentation of living phytoplankton provides a net gain to the detritus pool. The flux of algae across the bottom boundary is taken as a source term in the detritus equation (eq. (7)). The remineralized detritus is then transported back as phosphate and total inorganic nitrogen into the water column by upward diffusion. The latter mechanism is cast into the form of a boundary condition for the nutrient, which links the phosphate and nitrogen equations (eqs. (1) and (2)) with the detritus eq. (23).

$$D = \int_0^H \mathrm{SEDI}dz \quad \text{where} \quad \mathrm{SEDI} = (1-p_p)\mathrm{MOR}_P +$$
$$+(1-p_f)\{\mathrm{FEC}_T + \mathrm{FEC}_B\} + (1-p_z)\{\mathrm{MOR}_T + \mathrm{MOR}_B\}, \tag{49}$$
$$\mathrm{REMD} = r_d\{Detr\}. \tag{50}$$

2.2.7. Initial and boundary conditions

The following initial and boundary conditions supplement equation system (1)–(10): the initial vertical distributions of nutrient, phytoplankton, zooplankton, early juvenile of fish and detritus pool are known:

$$\begin{aligned}
\{Phyt\}(z,0) &= \{Phyt\}_0(z) && 0 \le z \le H\\
\{Z_{micro}\}(z,0) &= \{Z_{micro}\}_0(z) && 0 \le z \le H\\
Z_i(z,0) = Z_i^0(z), \quad W_i(z,0) &= W_i^0(z) && 0 \le z \le H\\
\{Z_{meso}\}(z,0) &= \sum_1^6 W_i^0 Z_i^0 &&\\
\{B\}(z,0) &= B_1(z) && 0 \le z \le H\\
\{Nutr_P\}(z,0) &= \{Nutr_P\}_0(z) && 0 \le z \le H\\
\{Nutr_N\}(z,0) &= \{Nutr_N\}_0(z) && 0 \le z \le H\\
\{Detr\}(t=0) &= \{Detr\}_0 = 0 && z = H.
\end{aligned} \tag{51}$$

The vertical gradients of phytoplankton, zooplankton and nutrient concentration flux are zero at the sea surface ($z = 0$):

$$F_{Phyt}(0) \equiv K_z \frac{\partial\{Phyt\}(z,t)}{\partial z}\bigg|_{z=0} - w_z\{Phyt\}(0,t) = 0, \tag{52}$$

$$\begin{aligned}
F_{Nutr_P}(0) &\equiv K_z \frac{\partial\{Nutr_P\}(z,t)}{\partial z}\bigg|_{z=0} = 0\\
F_{Nutr_N}(0) &\equiv K_z \frac{\partial\{Nutr_N\}(z,t)}{\partial z}\bigg|_{z=0} = 0,
\end{aligned} \tag{53}$$

$$\begin{aligned}
F_{Z_{micro}}(0) &\equiv K_z \frac{\partial\{Z_{micro}\}(z,t)}{\partial z}\bigg|_{z=0} = 0\\
F_{Z_{meso}}(0) &\equiv K_z \frac{\partial\{Z_{meso}\}(z,t)}{\partial z}\bigg|_{z=0} = 0\\
F_B(0) &\equiv K_z \frac{\partial\{B\}(z,t)}{\partial z}\bigg|_{z=0} = 0.
\end{aligned} \tag{54}$$

However, the bottom flux condition for phytoplankton, nutrient and zooplankton is given by:

$$F_{Phyt}(H) \equiv -w_z\{Phyt\}(H,t), \tag{55}$$

$$\begin{aligned} F_{Nutr_P}(H) &\equiv K_z \frac{\partial\{Nutr_P\}(z,t)}{\partial z}\bigg|_{z=H} = g_P\mathrm{REMD} \\ F_{Nutr_N}(H) &\equiv K_z \frac{\partial\{Nutr_N\}(z,t)}{\partial z}\bigg|_{z=H} = g_N\mathrm{REMD}, \end{aligned} \tag{56}$$

$$\begin{aligned} F_{Z_{micro}}(H) &\equiv K_z \frac{\partial\{Z_{micro}\}(z,t)}{\partial z}\bigg|_{z=H} = 0 \\ F_{Z_{meso}}(H) &\equiv K_z \frac{\partial\{Z_{meso}\}(z,t)}{\partial z}\bigg|_{z=H} = 0 \\ F_B(0) &\equiv K_z \frac{\partial\{B\}(z,t)}{\partial z}\bigg|_{z=H} = 0. \end{aligned} \tag{57}$$

This flux $F_P(H)$ enters the benthic detritus equation (eq. (7)) as a source term. The boundary condition (eq. (56)) provides the mechanism by which the water column is replenished with nutrients derived from benthic remineralization.

2.3. Physical submodel

Here, the proposed model is more complex than the usual frictional model and takes the form of a turbulence closure scheme; details can be found in Chapter 4 in Dyke (2001). As there is no need to include the troublesome non-linear terms, the governing equations take the forms in eqs. (58)–(60) (see Friedrich et al. 1981, Kochergin 1987). The Coriolis force is maintained to enable layer dynamics. Both velocities are affected by turbulent diffusion and Coriolis acceleration. The temperature changes are caused by turbulent heat diffusion, solar heating of the water column and surface heat fluxes:

$$\frac{\partial u}{\partial t} - fv = \frac{\partial}{\partial z}\left(A_z\frac{\partial u}{\partial z}\right), \tag{58}$$

$$\frac{\partial v}{\partial t} + fu = \frac{\partial}{\partial z}\left(A_z\frac{\partial v}{\partial z}\right), \tag{59}$$

$$\frac{\partial T}{\partial t} = \frac{\partial}{\partial z}\left(A_z\frac{\partial T}{\partial z} - \frac{1}{c\rho_0}Q_g\exp(-K_d z)\right), \tag{60}$$

where, as usual, u and v are the easterly and northerly components of the velocity, f is the Coriolis parameter, z is vertically upward component, t is time and A_z is the vertical eddy coefficient for momentum and heat. K_d is the mean extinction coefficient and c is the specific heat of sea water. K_d is the sum of the components responsible for the attenuation of irradiance by pure water, phytoplankton and other optically active admixtures, which was calculated from Woźniak's bio-optical classification of natural waters (Woźniak & Pelevin 1991) (see eq. (17)). The last term in the temperature equation is the heat source term, representing the effect of solar radiation in the water. Usually the exponential decay of underwater radiation is assumed. The vertical eddy coefficient for momentum and heat is obtained by the relationship (Peters et al. 1988)

$$A_z = 5 \times 10^{-4}(1 + R_i)^{-1.5} + 2 \times 10^{-6}. \tag{61}$$

The relationships $R_i = N^2/[(\frac{\partial u}{\partial z})^2 + (\frac{\partial v}{\partial z})^2]$, where R_i is the Richardson number, and N is the Brunt-Väisälä frequency $N = \frac{-g}{\rho}\frac{\partial \rho}{\partial z}$, relate these dimensionless numbers to the velocity and the density. The latter is in turn related to temperature through the equation $\rho = \rho_o(1 - \alpha T)$, in which α is the constant thermal expansion coefficient. A list of the symbols used in the physical model is given in Appendix 2.

2.3.1. Boundary conditions

The boundary conditions for momentum transfer across the sea surface ($z = 0$) are

$$F_u(0) \equiv A_z\frac{\partial u}{\partial z} = -\frac{\tau_x}{\rho_o}, \quad F_v(0) \equiv A_z\frac{\partial v}{\partial z} = -\frac{\tau_y}{\rho_o}, \tag{62}$$

where τ_x, τ_y are the components of the surface wind stress vectors in the x- and y- directions respectively.

The total heat flux Q at the sea surface is transmitted in accordance with:

$$F_Q(0) \equiv c\rho_o A_z\frac{\partial T}{\partial z} = Q. \tag{63}$$

At the bottom ($z = H$) the velocity components and the heat flux vanish:

$$u = v = 0, \quad \frac{\partial T}{\partial z} = 0. \tag{64}$$

The wind stress components at the sea surface (τ_x, τ_y) are calculated using standard formulas (Lehmann 1995):

$$\tau_x = \rho c_D u_x U_a, \quad \tau_y = \rho c_D u_y U_a, \tag{65}$$

with the drag coefficient c_D according to Large & Pond (1981):

$$c_D 10^3 = \begin{cases} 1.14 & \text{if } \; U_a \leq 10 \text{ m s}^{-1} \\ (0.49 + 0.065 U_a) & \text{if } \; 10 \text{ m s}^{-1} \leq U_a \leq 25 \text{ m s}^{-1}, \end{cases} \tag{66}$$

where U_a, u_x, u_y – absolute value (module) and components of the 'real' wind vector at the standard height above the free sea surface.

2.4. Meteorological submodel

For the physical submodel, the wind stress (see eq. (65)), the heat and radiative fluxes (see equations below) are needed at the sea surface.

The local heat flux through the sea surface Q is estimated from a simplified version of the heat budget of the sea surface. Hence, the local flux of thermal energy Q consists of the direct and diffusive solar (= global) radiation Q_g, net long-wave radiation flux Q_B, sensible heat flux Q_S and latent heat flux Q_L:

$$Q = Q_g - Q_B + Q_S + Q_L. \tag{67}$$

The modelled global radiation at the sea surface, Q_g, is expressed by the relation (Atwater & Ball 1978, Krężel 1985, Rozwadowska 1991, Rozwadowska & Isemer 1998):

$$Q_g = \frac{S f (T_i - A_{wa}) T_{aer} T_{cl} \cos\vartheta}{1 - A_{sk} A_s}, \tag{68}$$

where the factor describing the seasonal changes in the solar constant due to changes in the Sun-Earth distance f is given by Paltridge & Platt (1976), the transmittance for an ideal atmosphere $T_i(\vartheta, p)$ by Atwater & Brown (1974), the absorbance of water vapour $A_{wa}(e_0, \vartheta)$ by McDonald (1960), the aerosol transmittance function $T_{aer}(\vartheta, month, \phi, \lambda)$ by Rozwadowska (1991), and the sky $A_{sk}(c, cc)$ and sea surface albedos $A_s(T_{atm}, \vartheta, ice)$ by Rozwadowska (1991), Kamada & Flocchini (1986) and Isemer (1998). Q_g also depends on the solar zenith angle, $\vartheta(t_{UTC}, d, \phi, \lambda)$ (see Rozwadowska 1991).

The net long-wave radiation flux of the sea surface Q_B in the southern Baltic Sea is calculated from the formula (Woźniak et al. 2001):

$$\begin{aligned} Q_B \;\; = \;\; & 0.98\,\sigma T_s^4 - \sigma T_a^4 (0.732(1 - \exp(-0.47 e_s)) \\ & (1 - 0.067C + 0.301C^2)), \end{aligned} \tag{69}$$

where σ is the Stefan-Boltzmann constant ($5.673 \times 10^{-8}\,\mathrm{W\,m^{-2}K^{-4}}$), T_s is the sea surface temperature, T_a is the air temperature (in K), e_s is the surface water vapour pressure (in mb).

The net sensible and latent heat fluxes, Q_S and Q_L, are calculated by the expressions eqs. (70) and (71) with the latent heat of vaporization, L_P, (eq. (72)) and the respective transfer coefficients for heat and humidity, C_S and C_L, parameterized by the method of Launiainen (1979) (see also Jankowski & Masłowski 1991) (eq. (73)):

$$Q_S = \rho_a \, c_{pa} \, U_a \, C_S (t_s - t_a), \tag{70}$$

$$Q_L = U_a \, C_L \, L_P \, \frac{1}{R} \left(\frac{e_s}{T_s} - \frac{e_a}{T_a} \right), \tag{71}$$

where

$$e_s(t_s) \;=\; e_a(t) + 0.000678(1 + 0.00115 \, t_s) \, p_a (t_a - t_s)$$

$$L_P \;=\; 2500775.6 - 2360.10 \, t_a, \tag{72}$$

$$C_S = C_L = (0.041 \, U_a + 1.0698) \times 10^{-3}, \tag{73}$$

where c_{pa} is the specific heat capacity of air (c_{pa} = 57.6 J kg^{-10} C^{-1}), t_s, t_a are the sea water and air temperatures in °C, e_s is the water vapour pressure and e_a is the vapour pressure of the air (in Pa), p_a is the atmospheric pressure at the sea surface, R = 461.51 J kg^{-1} K^{-1} the gas constant for water vapour, U_a is the wind velocity at 10 m height in ms^{-1}.

3. Conclusion

At present one of the most important aspects of oceanological studies is monitoring the state and bioproductivity of marine ecosystems. Bioproductivity plays a considerable role in local and global changes. These are difficult to assess, demanding as they do a knowledge of the mechanisms affecting biological production and the functional relations between physiological processes in zooplankton species, as well as an understanding of environmental parameters in the sea and how they influence the food chain. Deterministic mathematical models are effective tools in solving problems concerning the bioproductivity of ecosystems.

In the past, where zooplankton has been introduced into a model, factors such as filtering, respiration, and excretion rates have often been taken as fixed productions of the hypothetical biomass rather than being related to more detailed information on behaviour and metabolism. The literature provides ample experimental data on these factors for several species of zooplankton. This information can be applied to gain some idea of the functional relationships potentially useful in simulating the response of zooplankton to variations in their environment (Dzierzbicka-Głowacka 2004a,b, Dzierzbicka-Głowacka & Zieliński 2004). The elaboration of such theoretical descriptions is critical to the inclusion of these animals, as animals, in more general simulations of ecosystems.

The work presents the idea of a one-dimensional Coupled Ecosystem Model with a high-resolution module for mesozooplankton – a copepod model, and a simple prey-predator model. In this model the mesozooplankton (herbivorous copepods) is treated not as a biomass but as organisms having definite patterns of growth, reproduction and mortality. It is assumed that only one species of copepod (*P. elongatus*) is present. However, the predator is introduced as a top regulator and is represented by early juvenile herring *C. harengus*.

This work is an attempt at synthesizing basic physical and biological processes in the marine environment and the links between them, mainly for their mathematical considerations, but especially for numerical modelling.

The system of equations with initial and boundary conditions has been solved numerically using the indirect Crank-Nicholson method (Potter 1982) in a layer $0 \leq z \leq H$ by digitizing this region with a variable vertical step. This method is absolutely convergent and is characterized by a second-order accuracy with respect to time and space discretization. The detailed algorithm of the solution to the model can be found in Dzierzbicka-Glowacka (2000).

The main aim of this paper, i.e. to construct the meteorological-physical-biological model, was achieved by working out:

- the model of the solar energy inflow into water surface,
- the dynamic model of the movement of water masses, and
- the biological model determining the vertical changes in time in the distributions of the nutrient concentration and phytoplankton, microzooplankton and mesozooplankton and early juvenile herring biomass.

The $1D$-Coupled Ecosystem Model is an open model which enables the study of: (1) annual, seasonal, monthly and daily variability of marine plankton in the southern Baltic Sea, (2) the impact of various climatic conditions over several years, and (3) the influence of different hydrophysical and biological processes on the vertical distributions of characteristics as a function of time.

The $1D$-CEM model presented in this paper may have a practical use in forecasting ecological changes in the Baltic.

This model was also tested, and the numerical simulations done for one year (1999) at a station in the southern Baltic Sea are presented in Part 2. The dynamic constants used in this model were determined mostly from data derived from the literature. The selected values of the parameters were reasonably close to the levels found in Baltic waters. Such an approach to the problem permits a detailed description of the quantities and variability of marine plankton on the basis of 3-hourly meteorological standard observations.

References

Atwater M. A., Ball J. T., 1978, *A numerical solar radiation model based on standard meteorological observations*, Sol. Energy, 21 (3), 163–170.

Atwater M. A., Brown P. S., 1974, *Numerical computations of the latitudinal variation of solar radiation for an atmosphere of varying opacity*, J. Appl. Meteorol., 13, 289–297.

Billen G., Lancelot C., Meybeck M., 1991, *N, P and Si retention along the aquatic continuum from land to ocean*, [in:] *Ocean margin processes in global change, physical, chemical, and earth sciences research*, R. F. C. Mantoura, J. M. Martin & R. Wollast (eds.), Wiley & Sons, New York, 19–44.

Caparroy P., Carlotti F., 1996, *A model for Acartia tonsa: effect of turbulence and consequences for the related physiological processes*, J. Plankton Res., 18 (11), 2139–2177.

Carlotti F., Radach G., 1996, *Seasonal dynamics of phytoplankton and Calanus finmarchicus in the North Sea as revealed by a coupled one-dimensional model*, Limnol. Oceanogr., 41 (3), 522–539.

Carlotti F., Wolf K. U., 1998, *A Lagrangian ensemble model of Calanus finmarchicus coupled with a 1-D ecosystem model*, Fish. Oceanogr., 7 (3)–(4), 191 –204.

Corkett C. J., McLaren I. A., 1978, *The biology of Pseudocalanus*, Adv. Mar. Biol., 15, 1–231.

Dower J., Miller T. J., Leggett W. C., 1997, *The role of microscale turbulence in the feeding ecology of larval fish*, Adv. Mar. Biol., 31, 169–220.

Dzierzbicka-Głowacka L., 2000, *Mathematical modelling of the biological processes in the upper layer of the sea*, Diss. and monogr., Inst. Oceanol. PAS, Sopot, 13, 124 pp., (in Polish).

Dzierzbicka-Głowacka L., 2004a, *Growth and development of copepodite stages of Pseudocalanus spp*, J. Plankton Res., 26 (1), 49–60.

Dzierzbicka-Głowacka L., 2004b, *The dependence of body weight in copepodite stages of Pseudocalanus spp. on variations of ambient temperature and food concentration*, Oceanologia, 46 (1), 45–63.

Dzierzbicka-Głowacka L., 2005, *A numerical investigation of phytoplankton and Pseudocalanus elongatus dynamics in the spring bloom time in the Gdańsk Gulf*, J. Marine Syst., 53 (1)–(4), 19–36.

Dzierzbicka-Głowacka L., *Encounter rate in plankton*, Pol. J. Environ. Stud., 15 (2), (in press).

Dzierzbicka-Głowacka L., *Equivalence of rates of growth and egg production of Pseudocalanus*, Ocean. Hydrobiol. Stud., 24 (4), 19–32, (in press).

Dzierzbicka-Głowacka L., Zieliński A., 1997a, *Numerical studies of the influence of the nutrient regeneration mechanism on the chlorophyll a concentration in a stratified sea*, Oceanologia, 39 (1), 55–82.

Dzierzbicka-Głowacka L., Zieliński A., 1997b, *Numerical studies of the influence of the benthic detritus pool on the chlorophyll a concentration in a stratified sea*, Oceanologia, 39 (4), 339–376.

Dzierzbicka-Głowacka L., Zieliński A., 2004, *Potential rate of reproduction for some geographically separate populations of Pseudocalanus spp*, Oceanologia, 46 (1), 65–83.

Dyke P. G., 2001, *Coastal and shelf sea modelling*, Kluwer Acad. Publ., Boston, 257 pp.

Ennet P., Kinnunen K., Tamsalu R., 1989, *Ecosystem model FINEST*, Valgus, Tallinn, 89 pp.

Evans G. T., 1989, *The encounter speed of moving predator and prey*, J. Plankton Res., 11, 415–417.

Fennel W., 2001, *Modeling of copepods with links to circulation model*, J. Plankton Res., 23 (11), 1217–1232.

Fennel W., Neumann T., 2003, *Variability of copepods as seen in a coupled physical biological model of the Baltic Sea*, ICES Mar. Sci. Symp., 219, 208–219.

Fey D. P., 2001, *Differences in temperature conditions and somatic growth rate of larval and early juvenile spring-spawned herring from the Vistula Lagoon, Baltic Sea, manifested in the otolith to fish size relationship*, J. Fish. Biol., 58 (8), 1257–1273.

Fonselius S. H., 1969, *Hydrography of the Baltic deep basins. III. Fishery Board of Sweden*, Ser. Hydrogr. Rep. No 23, 1–97.

Fransz H. G., Gonzalez S. R., Steeneken S. F., 1998, *Metazoan plankton and the structure of the plankton community in the stratified North Sea*, Mar. Ecol. Prog. Ser., 175, 191–200.

Fransz H. G., Mommaerts J., Radach G., 1991, *Ecological modelling of the North Sea*, Neth. J. Sea Res., 28 (1)–(2), 67–140.

Friedrich H. J., Kochergin V. P., Klimok V. I., Protasov A. V., Sukhorukov V. A., 1981, *Numerical experiments for the model of the upper oceanic layer*, Meteorol. Gidrol., 7, 77–85.

Isemer H.-J., 1998, *Sea ice concentration at the Baltic Proper – A digital 1 data set for 1964 to 1995*, Proc. 2nd Study Conf. BALTEX, Juliusruh, Island of Rügen, Germany, 25–29 May 1998, E. Raschke & H.-J. Isemer (eds.), Int. BALTEX Sec. Publ. Ser., 11, 78–79.

Jankowski A., Masłowski W., 1991, *Methodological aspects of wind momentum, heat and moisture fluxes evaluation from the standard hydrometeorological measurements on board a ship*, Stud. Mater. Oceanol., 58 (1), 63–76.

Jansson B., 1972, *Ecosystem approach to the Baltic problem*, Bull. Ecol. Res. Com. NFR, 16, 1–82.

Jędrasik J., Kowalewski M., 1993, *Transport model of pollutants in the Gulf of Gdańsk*, Stud. Mater. Oceanol., 64 (3), 61–75.

Kamada R. F., Flocchini R. G., 1986, *Gaussian solar flux model*, Sol. Energy, 36 (1), 73–87.

Kiørboe T., 1993, *Turbulence, phytoplankton cell size, and the structure of pelagic food webs*, Adv. Mar. Biol., 29, 1–72.

Kiørboe T., MacKenzie B. R., 1995, *Turbulence-enhanced prey encounter rates in larval fish: effects of spatial scale, larval behaviour and size*, J. Plankton Res., 17, 2319–2331.

Kiørboe T., Saiz E., 1995, *Planktivorous feeding in calm and turbulent environmants with emphasis on copepods*, Mar. Ecol. Prog. Ser., 122, 135–145.

Klein Breteler W. C. M., Gonzalez S. R., Schogt N., 1995, *Development of Pseudocalanus elongatus (Copepoda, Calanoida) cultured at different temperature and food conditions*, Mar. Ecol. Prog. Ser., 119, 99–110.

Kochergin V. P., 1987, *Three-dimensional prognostic models*, [in:] *Three-dinensional Coastal Ocean Models*, N. S. Heaps (ed.), Am. Geophys. Union, Coast. Estuar. Sci. Ser., 4, 201–208.

Krężel A., 1985, *Solar radiation at the Baltic Sea surface*, Oceanologia, 21, 5–32.

Large W. G., Pond S., 1981, *Sensible and latent heat flux measurements over the ocean*, J. Phys. Oceanogr., 12 (5), 464–482.

Laurence G. C., 1985, *A report on the development of stochastic models of food-limited growth and survival in cod and haddock larvae on Georges Bank*, [in:] *Growth and survival of larval fishes in relation to the trophodynamics of Georges Bank cod and haddock*, G. C. Laurence & R. G. Lough (eds.), NOAA Tech. Mem., NMFS-F/NEC-36, 83–150.

Lehmann A., 1995, *A three-dimensional baroclinic eddy-resolving model of the Baltic Sea*, Tellus, 47 (A), 1013–1031.

MacKenzie B. R., Kiørboe T., 1995, *Encounter rates and swimming behaviour of pause-travel and cruise larval fish predators in calm and turbulent laboratory environments*, Limnol. Oceanogr., 40 (T), 1278–1289.

Margoński P., 2000, *The abundance, growth rate and mortality of the early life stages of herring (Clupea harengus) and smelt (Osmerus eperlanus) in the Vistula Lagoon (southern Baltic Sea) during 1998–1999*, ICES CM, N:21.

Marmefelt E., Lennart F., Ivarsson M., 2002, Final Environmental Status Report 2000 for the Baltic Sea, SMHI, [http://www.imr.no/morten/nocomments/publications/nowcast2000 Smhi.pdf].

McDonald J. E., 1960, *Direct absorption of solar radiation by atmospheric water vapour*, J. Meteorol., 17, 319–328.

Miller T. J., Crowder L. B., Rice J. A., Marschall E. A., 1988, *Larval size and recruitment mechanisms in fishes: toward a conceptual framework*, Can. J. Fish. Aquat. Sci., 45, 1657–1670.

Ołdakowski B., Renk H., 1997, *The conception and structure of the production –destruction of organic matter model; verification tests for the Gulf of Gdańsk*, Oceanol. Stud., 26 (4), 99–122.

Paffenhöfer G. A., 1971, *Grazing and ingestion rates of nauplii, copepodids and adults of the marine planktonic copepod Calanus helgolandicus*, Mar. Biol., 11, 286–298.

Paltridge G.W., Platt C.M.R., 1976, *Radiative processes in meteorology and climatology*, Elsevier, Amsterdam, 318 pp.

Parsons T.R., Tokahashi M., Hargrave B., 1977, *Biological oceanographic processes*, 2nd edn., Pergamon Press, Oxford, 332 pp.

Parsons T.R., Tokahashi M., Hargrave B., 1984, *Biological oceanographic processes*, 3rd edn., Pergamon Press, Oxford, 330 pp.

Peters H., Gregg M.C., Toole J.M., 1988, *On the parametrization of equatorial turbulence*, J. Geophs. Res., 93 (C2), 1199–1218.

Potter D., 1982, *Computation physics*, Vol. 1, Wiley, New York, 278 pp.

Radach G., Berg J., Heinemann B., Krause M., 1984, *On the relation of primary production and herbivorous zooplankton grazing in the northern North Sea during FLEX'76*, [in:] *Flows of energy and materials in marine ecosystems, theory and practice*, M. Fasham (ed.), NATO Conf. Ser. 4, Plenum Press, New York, 597–625.

Radach G., Moll A., 1993, *Estimation of the variability of production by simulating annual cycles of phytoplankton in the central North Sea*, Prog. Oceanogr., 31, 339–419.

Raymont J.E.G., 1980, *Plankton and productivity in the oceans*, Vol. 1. *Phytoplankton*, Pergamon Press, Oxford, 489 pp.

Renk H., Ochocki S., 1998, *Photosynthetic rate and light curves of phytoplankton in the southern Baltic*, Oceanologia, 40 (4), 331–344.

Riley G.A., 1946, *Factors controlling phytoplankton populations on Georges Bank*, J. Mar. Res., 6, 54–73.

Rothschild B.J., Osborn T.R., 1988, *Small-scale turbulence and plankton contact rates*, J. Plankton Res., 10 (3), 465–474.

Rozwadowska A., 1991, *A model of solar energy input into the Baltic Sea*, Stud. Mater. Oceanol., 59 (6), 223–242.

Rozwadowska A., Isemer H.-J., 1998, *Solar radiation fluxes at the surface of the Baltic Proper. Part 1. Mean annual cycle and influencing factors*, Oceanologia, 40 (4), 307–330.

Ryther J.H., 1956, *Photosynthesis in the ocean as a function of light intensity*, Limnol. Oceanogr., 1 (1), 61–70.

Savchuk O., Kolodochka A., Gutsabbath E., 1988, *Simulation of the matter cycle in the Baltic Sea ecosystem*, Proc. 16th Conf. Baltic Oceanogr, Kiel, 921–931.

Seuront L., Schmitt F., Lagadeuc Y., 2001, *Turbulence intermittency, small-scale phytoplankton patchiness and encounter rates in plankton: where do we go from here?*, Deep-Sea Res. Pt. I, 48 (5) 1199–1215.

Sjöberg S., 1980, *A mathematical and conceptual framework for models of the pelagic ecosystem of the Baltic Sea*, [in:] *Formulations and exploratory simulations*, Stockholm Univ., Stockholm, 27 pp.

Steele J.H., 1974, *The structure of marine ecosystems*, Harvard Univ. Press, Cambridge, 128 pp.

Steele J. H., Mullin M. M., 1977, *Zooplankton dynamics*, [in:] *The sea*, E. D. Goldberg, I. N. McCave, J. J. O'Brien & J. H. Steele (eds.), Intersci. Publ., New York, 6, 857–887.

Stigebrandt A., Wulff F., 1987, *A model for the dynamics of nutrients and oxygen in the Baltic Proper*, J. Mar. Res., 45, 729–759.

Sundby S., Fossum P., 1990, *Feeding conditions of Arcto-Norwegian cod larvae compared to the Rothschild-Osborn theory on small-scale turbulence and plankton contact rates*, J. Plankton Res., 12 (6), 1153–1162.

Svansson A., 1996, *A diffusion model for the primary production of phytoplankton*, Deep-Sea Res. Pt. II, 43 (1), 37–46.

Tamsalu R. (ed.), 1998, *Coupled 3D hydrodynamic and ecosystem model FinEst, FIMR*, Finn. Inst. Mar. Res., Rap. No 35, Helsinki, 166 pp.

Tamsalu R., Ennet P., 1995, *Ecosystem modelling in the Gulf of Finland. II. The aquatic ecosystem Model FINEST*, Estuar. Coast. Shelf Sci., 41 (4), 429–458.

Woźniak B., Pelevin V. N., 1991, *Optical classifications of the seas in relation to phytoplankton characteristics*, Oceanologia, 31, 25–55.

Woźniak S. B., Zapadka T., Woźniak B., 2001, *Comparison between various formulae for sea surface net long-wave radiation flux and a new empirical formula for the southern Baltic region*, Proc. 3rd Study BALTEX Conf., Aaland Islands (Finland), 2–6 July 2001, Int. BALTEX Secret., GKSS Res. Center., Geesthacht, 257–258.

Appendix 1

List of symbols used in the biological submodel

Symbol	Denotes	Unit
B	predator biomass	$\mathrm{mg\,C\ m^{-3}}$
d_A	assimilation number	$\mathrm{gC(g\,Chl\,h)^{-1}}$
d_I	light limitation factor	
d_P	phosphate limitation factor	
d_N	total inorganic nitrogen limitation factor	
d	predator reaction distance	cm
d_o	body length of predator	mm
$\{Detr\}$	detritus concentration	$\mathrm{gC\ m^{-2}}$
E_o	photosynthetically available irradiation PAR	$\mathrm{W\ m^{-2}}$
E_{opt}	saturation irradiance	$\mathrm{kJ\ m^{-2}\ h^{-1}}$
E	irradiance at depth z	$\mathrm{kJ\ m^{-2}\ h^{-1}}$
$E = E_B + E_T$	encounter rate	$\mathrm{s^{-1}}$
$f_{\max}$	maximum growth rate for Z_{micro}	$\mathrm{day^{-1}}$
$g_{\max}$	maximum grazing rate	$\mathrm{day^{-1}}$
g_N	N/C ratio	$\mathrm{mmol\,N\,(mg\,C)^{-1}}$
g_P	P/C ratio	$\mathrm{mmol\,P\,(mg\,C)^{-1}}$
g_{Chl}	C/Chl a ratio	$\mathrm{gC(gChl}\,a)^{-1}$
g_B	predator growth rate	$\mathrm{day^{-1}}$
g_1	proportionality parameter between growth rate and encounter rate	
g_2	constant growth rate term	$\mathrm{day^{-1}}$
$k_{Nutr\,N}$	half-saturation constant for total inorganic nitrogen	$\mathrm{mmol\,N\ m^{-3}}$
$k_{Nutr\,P}$	half-saturation constant for phosphate	$\mathrm{mmol\,P\ m^{-3}}$
k_{Phyt}	half-saturation constant for grazing	$\mathrm{mg\,C\ m^{-3}}$
K_z	turbulent diffusion coefficient	$\mathrm{m^2\ s^{-1}}$
l	characteristic length scale of turbulent eddies	m
m_P^n	percentage of basic respiration	
m_P^d	percentage of photorespiration	
m_P	mortality rate of $\{Phyt\}$	$\mathrm{day^{-1}}$
m_Z	mortality rate for $\{Z_{meso}\}$	$\mathrm{day^{-1}}$
n_e	percentage of ingestion regenerated as soluble excretion of zooplankton	
n_f	percentage of ingestion egested as faeces	
n_Z	material percentage of ingestion ending up as dead zooplankton	
$\{Nutr\}_N$	total inorganic nitrogen	$\mathrm{mmol\,N\ m^{-3}}$
$\{Nutr\}_P$	phosphate concentration	$\mathrm{mmol\,P\ m^{-3}}$
p_f	percentage of remineralized faecal material in the water column	

List of symbols used in the biological submodel (*continued*)

Symbol	Denotes	Unit
p_p	percentage of remineralized dead organic matter in the water column	
p_z	percentage of remineralized dead zooplankton in the water column	
$\{Phyt\}_0$	phytoplankton threshold for grazing	mg Cm^{-3}
$\{Phyt\}$	phytoplankton biomass	mg C m^{-3}
r_d	remineralizaton rate of benthic detritus	day^{-1}
t_1	temperature coefficient	
t_2	temperature coefficient	
t_o	time in which the maximum zooplankton concentration occurs	
w	encounter turbulent velocity	m s^{-1}
W_{female}	female weight	$\mu g_{w.w}$
W_{egg}	egg weight	$\mu g_{d.w}$
W_i	weights of i cohorts	μgC
Z_i	numbers of i cohorts	m^{-3}
$\{Z_{micro}\}$	microzooplankton biomass	mg C m^{-3}
$\{Z_{meso}\}$	mesozooplankton biomass	mg C m^{-3}
X	efficiency term	
τ	coefficient of food selction	
ε	dissipation rate of turbulent kinetic energy	m^2 s^{-1}

Appendix 2

List of symbols used in the physical submodel

Symbol	Denotes	Unit
A_z	turbulent diffusion coefficient	m^2 s^{-1}
c	specific heat of sea water	kcal kg^{-10} C^{-1}
f	Coriolis parameter	s^{-1}
T	temperature	°C
U_a	wind velocity	m s^{-1}
u	water velocity in the x-direction	m s^{-1}
v	water velocity in the y-direction	m s^{-1}
Q_I	global radiation	W m^{-2}
Q_B	back radiation	W m^{-2}
Q_L	latent heat flux	W m^{-2}
Q_S	sensible heat flux	W m^{-2}
τ_x	wind stress in the x-direction	kg s^{-2}
τ_y	wind stress in the y-direction	kg s^{-2}
ρ	water density	kg m^{-3}